ChemComm

Ferrocene Metallopolymers of Intrinsic Microporosity (MPIMs)

Journal:	*ChemComm*
Manuscript ID	CC-COM-09-2021-005022.R2
Article Type:	Communication

ARTICLE

Ferrocene Metallopolymers of Intrinsic Microporosity (MPIMs)

Tianran Zhai,[a] Kenson Ambrose, Audithya Nyayachavadi, Kelly G. Walter,[c] Simon Rondeau-Gagné,[b] and Jeremy I. Feldblyum*[a]

Received 00th January 20xx,
Accepted 00th January 20xx

DOI: 10.1039/x0xx00000x

We show here that non-network metallopolymers can possess intrinsic microporosity stemming from contortion introduced by metallocene building blocks. Metallopolymers constructed from ferrocenyl building blocks linked by phenyldiacetylene bridges are synthesized and possess BET surface areas up to 400 m^2/g. As solubility imparted by pendant groups reduces porosity, copolymerization is used to simultaneously improve both accessible surface area and solubility. Spectroscopic analysis provides evidence that mixed valency between neighboring ferrocenyl units is supported in these polymers.

Microporosity affords opportunities for unique and guest-dependent optical and electronic functionality.[1] However, the network (cross-linked) structure of most porous materials limits their solution processability and hence their utility in applications where high quality thin films are necessary, such as membrane-based separations, electronic devices, and energy storage.[2-4]

Polymers of intrinsic microporosity (PIMs),[5] in contrast to most[6] other microporous solids, are soluble in common organic solvents, allowing simple formation of high quality films by solution-casting methods.[7] While PIMs have achieved notable success for molecular sorption and separation,[7, 8] their optical and electronic properties remain largely unexplored – a consequence of the structural motifs most commonly used in PIMs, which lack backbone conjugation.[9] Several conjugated PIMs have been reported,[10-13] however, the backbone contortion that generates intrinsic microporosity in these polymers may also disrupt overlap between (intrachain) neighbouring π orbitals.

In this communication, we show that porosity, solubility, and intrachain electronic communication are not mutually exclusive. Main-chain metallopolymers rely on covalent or coordination bonds between metal and non-metal elements for the connectivity of the polymer chain. It is well-established that some of these polymers can support (semi)conductivity,[14] however, porosity in these linear (non-network) polymers has remained unstudied. In this work, we show that polymers based on aryleneethynylene-bridged ferrocene units can in fact be porous. We also demonstrate a delicate balance between porosity and solubility: these characteristics are not mutually exclusive, but require careful polymer design to achieve simultaneously. Finally, we show that, consistent with previous reports, intrachain electronic communication is supported in these polymers.

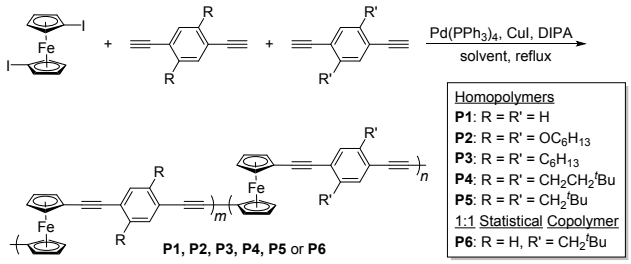

Scheme 1. Synthesis of ferrocene-based homopolymers and 1:1 statistical copolymer **P1**-**P6** by Pd-catalysed polycondensation.

Our rationale for choosing ferrocene-based polymers for this study was motivated by several factors. First, intrinsic microporosity in linear polymers is most easily generated by introducing sharp kinks in the chain backbone that prevent close-packing.[5, 15] We hypothesized that the low energy barrier to ferrocene-cyclopentadienyl (Cp) rotation would enable the desired sharp twists along the polymer backbone[16-18] to hinder close interchain packing. Second, as Cp rotation does not reduce molecular orbital overlap between ferrocene and its covalently bound, conjugated partners,[19, 20] we hypothesized that intrachain electronic communication would be supported regardless of Cp rotational states along the polymer backbone. Third, the synthesis of main-chain ferrocene polymers is well-established,[21, 22] providing a straightforward entry point to study potential porosity in these compounds.

Ferrocene aryleneethynylene polymers were prepared *via* Pd-catalysed polycondensation[23] as shown in Scheme 1. Following the method reported by Yamamoto's group,[24] substituted 1,4-diethynylbenzene monomers were coupled with 1,1-diiodoferrocene (FcI_2) by Sonogashira coupling[25, 26] (Scheme 1). Crude polymers were extracted, precipitated, and washed with organic solvents experimental details can be found

[a] *Department of Chemistry, The University at Albany, State University of New York, Albany, NY, 12222, United States. Email: jfeldblyum@albany.edu*
[b] *Department of Chemistry and Biochemistry, University of Windsor, Windsor, ON, N9B 3P4, Canada. Email: Simon.Rondeau-Gagne@uwindsor.ca*
[c] *Department of Microbiological Sciences, North Dakota State University, Fargo, ND, 58108*

Electronic Supplementary Information (ESI) available: Experimental details and characterisation including ^1H and ^{13}C NMR, infrared spectroscopy, N_2 gas sorption, thermogravimetric analysis, Raman spectroscopy, and cyclic voltammetry data. See DOI: 10.1039/x0xx00000x

in Section 1.3 of the Electronic Supporting Information (ESI)]. Table 1 summarizes the results of polymerization.

We began by synthesizing **P2**. Although this polymer was obtained relatively high yield (85%), precipitation of the polymer occurred soon after initiating polymerization. We hypothesized that termination of polymerization occurred due to the poor solubility of the polymer in the synthesis solvent (toluene). Furthermore, the formation of short chains due to rapid precipitation opposes our goal of achieving intrinsic microporosity, as we hypothesize that porosity increases with chain length (at least for short chains).[27] For this reason, we used dichloromethane (DCM) as the solvent for further polymerization. Indeed, the weight-average molecular weight (M_W) of **P3** obtained by high-temperature size exclusion chromatography (SEC) was significantly greater than that of the chemically similar **P2**. As the use of DCM was expected to lead to higher M_W, the higher M_Ws of polymers synthesized with DCM reduced their solubilities. Hence, analysis by SEC using 1,2,4-trichlorobenzene as the eluent at 180 °C led to a wide range of M_ws between 1.3 and 16.8 kDa, with the lowest values corresponding to the homopolymers empirically exhibiting the lowest solubilities (Table S7). The homopolymers with the greatest apparent solubilities in 1,2,4-trichlorobenzene, **P2** and **P3**, also exhibited the highest values of M_w (Table 1). The relatively narrow dispersities measured for these polymers is also consistent with our contention that solubility limits the measured M_ws, as step growth polymers should exhibit dispersity close to 2.[28] Artificially low dispersities can be obtained when only the lower molecular mass polymer fractions are dissolved.[29]

Analysis by ^{1}H NMR was also challenging due to the limited solubility of most of the homopolymers reported here. Analysis of **P4**, the polymer exhibiting the greatest solubility in $CDCl_3$, exhibited broad signals characteristic[30, 31] of polymers in solution (Fig. S17). The resonances at ca. 7 ppm, 4 ppm, and 1-2 ppm can be assigned to phenyl protons, Fc protons, and neohexyl protons, respectively. A weak resonance attributable to terminal –C≡H protons (ca. 3 ppm) was also observed. The integration ratio between these terminal protons and those of the Fc protons is 1:53, corresponding to an average degree of polymerization of 6.7, in reasonable agreement with that determined by SEC (5.3).

Analysis of **P1**-**P6** by Raman spectroscopy (Fig. 1) confirmed that all polymers contain the expected ν(C≡C) scattering peak of disubstituted acetylene[32, 33] at ca. 2200 cm^{-1}. The peaks in the 1500-1600 cm^{-1} range are assigned to symmetric stretches of the polymers' arylene segments.[34] The ν(C-H)[33] and ν(Fc-I)[35] vibrations, corresponding to terminal acetylene (~3300 cm^{-1}) and terminal FcI_2 (ca. 1140 cm^{-1} and 880 cm^{-1}) are not observable, consistent with a high degree of polymerization in these polymers.

Table 1. Preparation and properties of ferrocene polymers **P1**-**P6**.

Polymer	Method[a]	Yield	M_n[b] (kDa)	M_W[b] (kDa)	$Đ_M$	π-π* λ_{max} (nm)[c]	d-d λ_{max} (nm)[c]	IVCT λ_{max} (nm)[c]	HOMO-LUMO gap (eV)[c]
P1	B	46%	1.2	1.5	1.25	333	447	1642, 1669	1.35
P2	A	85%	5.9	6.5	1.10	333	443	1642	1.20
P3	A	49%	12.5	16.9	1.35	297	444	1642, 1711	1.54
P4	B	16%	2.5	2.9	1.16	313	453	1642, 1698	1.37
P5	B	35%	1.2	1.6	1.33	307	453	Not observed	1.04
P6	B	28%	11.1	16.5	1.49	292	452	1642, 1672	1.31

[a] Method A: 1.0 eq. of substituted 1,4-diethynylbenzene per 1.0 eq. of FcI_2 was added. Catalyst: 0.04 eq. $Pd(PPh_3)_4$ and 0.04 eq. of CuI per 1.0 eq. of the monomer. Base: excess of diisopropylamine (DIPA, 86 eq.). Method B: 1.0 eq. of substituted 1,4-diehtynylbenzene per 1.0 eq. of FcI_2 was added. Catalyst: 0.04 eq. $Pd(PPh_3)_4$ and 0.04 eq. of CuI per 1.0 eq. of the monomer. Base: 1.2 eq. DIPA. [b]Measured by high-temperature size exclusion chromatography in 1,2,4-trichlorobenzene at 180°C. [c]Determined from diffuse reflectance spectroscopy measurements.

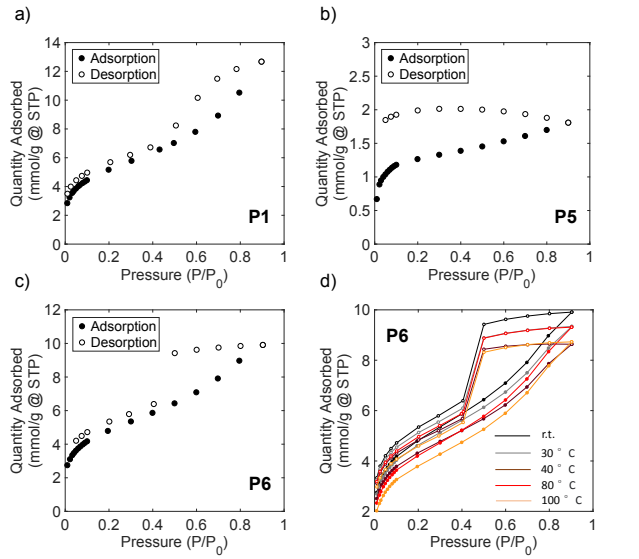

Fig. 2. (a) N_2 sorption isotherm of **P1** activated under reduced pressure (~200 mTorr) at r.t., (b) N_2 sorption isotherm of **P5** activated under reduced pressure (~200 mTorr) at r.t., (c) N_2 sorption isotherm of **P6** activated under reduced pressure (~200 mTorr) at r.t., and (d) N_2 sorption isotherms of **P6** activated under reduced pressure (~200 mTorr) at r.t, 30°C, 40°C, 80°C and 100°C.

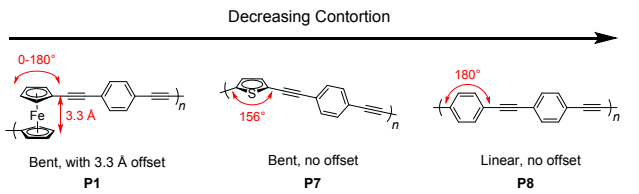

Scheme 2. Illustration of contortion introduced by using ferrocene in the polymer backbone, and control polymers synthesized to assess effect of contortion on polymer porosity.

N_2 gas sorption analysis was used to assess the porosity of the polymers studied herein. After activation from hexanes[36] at room temperature (r.t., ca. 23 °C), polymer **P1** exhibited a BET surface area of 416 m^2/g (Fig. 2a), despite its being a non-network polymer. The sharp rise in N_2 uptake at low pressure is consistent with microporosity, and the hysteresis loop between $P/P_0 = 0.4$ and 0.9 is consistent with some mesoporosity as well. Pore size distribution analysis of gas sorption data by density functional theory (Figs. S53 and S54) suggest that micropores of 6-13 Å diameter contribute to ca. 70% of the polymer's surface area. These results are consistent with our contention that main-chain ferrocene can sufficiently contort the polymer backbone to support intrinsic microporosity. Activation at higher temperatures led to negligible changes in accessible surface area (Table S1, Figs. S26-S30).

To assess the effect of main-chain ferrocene on the porosity of **P1**, we synthesized control polymers **P7** and **P8** (Scheme 2), which lack the chain segment offset introduced by ferrocene (**P7**) and both this offset and a bent polymer backbone (**P8**). When activated at r.t., the BET surface areas of **P7** and **P8** were determined to be 98 m^2/g and 160 m^2/g, respectively; activation at 100 °C led to respective BET surface areas of 65 m^2/g and 94 m^2/g (Figure S51). Hence, the high surface area observed for **P1** can be attributed specifically to polymer backbone contortion introduced by main-chain ferrocene.

Given the poor solubility of **P1**, we next examined potential porosity in polymers **P2** and **P3**. Gas sorption analysis showed that the addition of linear pendant groups led to the near-complete (for **P2**) and complete (for **P3**) elimination of measurable BET surface area (<10 m^2/g for our analysis conditions), regardless of activation method tested (Section S2.3, ESI). Likewise, the neohexyl-containing **P4** exhibited no measurable porosity. However, polymer **P5**, having the shortest pendant group tested (neopentyl), exhibited a BET surface area of 110 m^2/g after r.t. activation. Activation of **P5** at higher temperatures led to reductions in the BET surface area (Table S3 and Figs. S42-S43), presumably due to thermal degradation. Given the porosity of **P1** and the combination of both solubility and porosity of **P5**, the copolymer **P6** was synthesized from equimolar ratios of the monomers used to synthesize **P1** and **P5** (Scheme 1). **P6** exhibited a BET surface area of 391 m^2/g after r.t. activation and lower surface areas after higher temperature activation (Fig. 2d and Table S4). Furthermore, **P6** exhibited solubility similar to that of the homopolymer **P5** (Table S7).

The thermal behaviour of **P1**-**P6** was assessed by

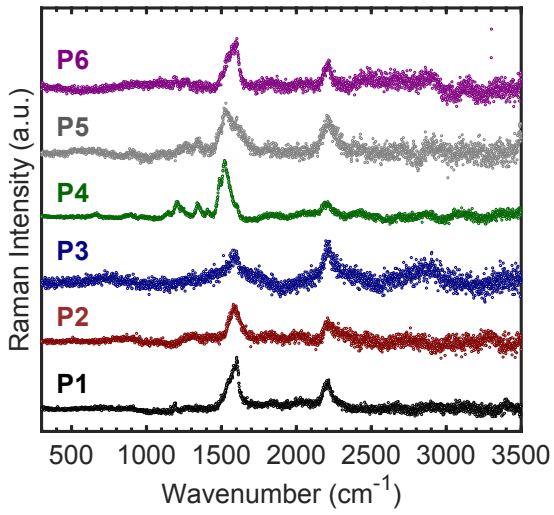

Fig. 1. Raman spectra of **P1**-**P6** corrected for fluorescence background. Raw data are shown in Fig. S60.

thermogravimetric analysis (Figs. S56-S61). Mass loss occurred around 350 °C for **P1** and **P4**. **P2** and **P3** began thermal decomposition around 220 °C, while decomposition began at a

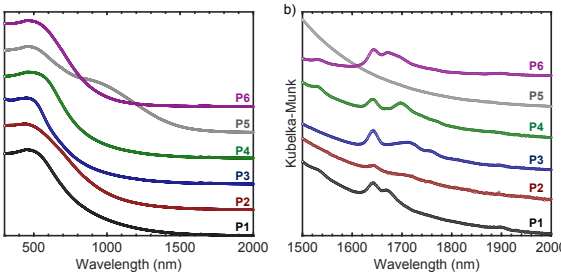

Fig. 3. a) UV-Vis-NIR diffuse reflectance spectra of **P1**-**P6** from 200-2200 nm. b) Detail of region from 1500-2000 nm (magnified 15x).

lower temperature (175 °C) for **P5** and **P6**. Mass spectrometry of the thermal decomposition products of **P4** (Fig. S62) showed

species of 39, 41, and 56 amu evolving from the polymer at ca. 400 °C, in accordance with the mass of isobutene (Fig. S64). This fragment may be formed by proton elimination of the *t*-butyl (propyl) cation generated from the decomposition of the ethyl-*t*-butyl pendant groups of the polymer. Similar evolution of isobutene at ca. 400 °C was observed for **P5** (Fig. S63).

Fig. 3 exhibits the solid-state UV-Vis-NIR diffuse reflectance spectra of **P1**-**P6**, and corresponding data are shown in Table 1. Absorption maxima at ca. 450 nm in Fig. 3 are assigned to the ferrocene d-d transition.[37-39] The π-π* adsorption band is present at ca. 310 nm,[24] and the HOMO-LUMO gaps of **P1**-**P6** range from 1.04 – 1.54 eV (Table 1). Cyclic voltammetry (CV) confirmed typical behaviour expected[24] for polyferrocenes (Figs. S66 and S67). UV-Vis-NIR was also used to assess evidence for mixed valency in the polymer, which can be important for intrachain charge transport.[40] Absorption between 1600-1700 nm, observed in all polymers except **P5**, is consistent with intervalence charge transfer (IVCT) bands seen in bridged diferrocenyl small molecules[37, 39] and is in accord with previous work[24] showing evidence of electron exchange between ferrocene backbone units in related ferrocenyl aryleneethynylene polymers. We attribute the lack of any distinct absorption feature in this wavelength range for **P5** to the poor thermal stability of this polymer. The presence of what appear to be multiple ICVT bands are tentatively attributed to the presence of distinct electronic environments within the polymer solid, although we cannot rule out the possibility of remote electron transfer[41] also contributing to NIR absorption.

In summary, we have shown that intrinsic microporosity in main-chain metallopolymers can be attributed to the organometallic constituents of the polymer backbone. Solubility and porosity, which appear to be inversely related in the ferrocene polymers studied here, can be simultaneously improved by copolymerization. These polymers can also exhibit electronic communication between ferrocene components in tandem with porosity and solubility. We term these porous, non-network metallopolymers "metallopolymers of intrinsic microporosity" (MPIMs).

T.Z., K.G.W., and J.I.F. gratefully acknowledge support from the Donors of the American Chemical Society Petroleum Research Fund (#59835-DNI10) and start-up funds from The University at Albany, State University of New York. The mass spectrometer-coupled thermogravimetric analyzer was supported by National Science Foundation Major Research Instrumentation grant #1919810. S.R.-G. would like to thank the financial support from Natural Sciences and Engineering Research Council of Canada (NSERC) through a Discovery Grant (RGPIN-2017-06611) and by the Canadian Foundation for Innovation (CFI). A.N. thanks NSERC for a doctoral scholarship.

Conflicts of interest

There are no conflicts to declare.

Notes and references

1. L. S. Xie, G. Skorupskii and M. Dincă, *Chem. Rev.*, 2020, **120**, 8536-8580.
2. H. B. Park, J. Kamcev, L. M. Robeson, M. Elimelech and B. D. Freeman, *Science*, 2017, **356**.
3. W.-T. Koo, J.-S. Jang and I.-D. Kim, *Chem*, 2019, **5**, 1938-1963.
4. L. Sun, M. G. Campbell and M. Dincă, *Angew. Chem., Int. Ed.*, 2016, **55**, 3566-3579.
5. N. B. McKeown, *ISRN Mater. Sci.*, 2012, **2012**, 513986.
6. Some porous molecular materials are soluble (M. A. Little and A. I. Cooper, *Adv. Funct. Mater.*, 2020, **30**, 1909842).
7. D. Fritsch, P. Merten, K. Heinrich, M. Lazar and M. Priske, *J. Membr. Sci.*, 2012, **401-402**, 222-231.
8. M. Lanč, K. Pilnáček, C. R. Mason, P. M. Budd, Y. Rogan, R. Malpass-Evans, M. Carta, B. C. Gándara, N. B. McKeown, J. C. Jansen, O. Vopička and K. Friess, *J. Membr. Sci.*, 2019, **570-571**, 522-536.
9. P. M. Budd, B. S. Ghanem, S. Makhseed, N. B. McKeown, K. J. Msayib and C. E. Tattershall, *Chem. Commun.*, 2004, 230-231.
10. G. Cheng, T. Hasell, A. Trewin, D. J. Adams and A. I. Cooper, *Angew. Chem., Int. Ed.*, 2012, **51**, 12727-12731.
11. G. Cheng, B. Bonillo, R. S. Sprick, D. J. Adams, T. Hasell and A. I. Cooper, *Adv. Funct. Mater.*, 2014, **24**, 5219-5224.
12. P. Klein, H. J. Jötten, C. M. Aitchison, R. Clowes, E. Preis, A. I. Cooper, R. S. Sprick and U. Scherf, *Polym. Chem.*, 2019, **10**, 5200-5205.
13. A. C. B. Rodrigues, I. S. Geisler, P. Klein, J. Pina, F. J. H. Neuhaus, E. Dreher, C. W. Lehmann, U. Scherf and J. S. Seixas de Melo, *J. Mater. Chem. C*, 2020, **8**, 2248-2257.
14. J.-C. Eloi, L. Chabanne, G. R. Whittell and I. Manners, *Materials Today*, 2008, **11**, 28-36.
15. N. B. McKeown, *International Scholarly Research Notices*, 2012, **2012**.
16. Y. Sha, H. Zhang, Z. Zhou and Z. Luo, *Polym. Chem.*, 2021, **12**, 2509-2521.
17. B. H. Jones, D. R. Wheeler, H. T. Black, M. E. Stavig, P. S. Sawyer, N. H. Giron, M. C. Celina, T. N. Lambert and T. M. Alam, *Macromolecules*, 2017, **50**, 5014-5024.
18. K. Kulbaba, I. Manners and P. M. Macdonald, *Macromolecules*, 2002, **35**, 10014-10025.
19. S. A. Getty, C. Engtrakul, L. Wang, R. Liu, S.-H. Ke, H. U. Baranger, W. Yang, M. S. Fuhrer and L. R. Sita, *Phys. Rev. B*, 2005, **71**, 241401.
20. M. Camarasa-Gómez, D. Hernangómez-Pérez, M. S. Inkpen, G. Lovat, E. D. Fung, X. Roy, L. Venkataraman and F. Evers, *Nano Lett.*, 2020, **20**, 6381-6386.
21. P. Nguyen, P. Gómez-Elipe and I. Manners, *Chem. Rev.*, 1999, **99**, 1515-1548.
22. R. D. A. Hudson, *J. Organomet. Chem.*, 2001, **637-639**, 47-69.
23. K. Sonogashira, Y. Tohda and N. Hagihara, *Tetrahedron Lett.*, 1975, **16**, 4467-4470.
24. T. Yamamoto, T. Morikita, T. Maruyama, K. Kubota and M. Katada, *Macromolecules*, 1997, **30**, 5390-5396.
25. R. Severin, J. Reimer and S. Doye, *J. Org. Chem.*, 2010, **75**, 3518-3521.
26. Z. Novák, A. Szabó, J. Répási and A. Kotschy, *J. Org. Chem.*, 2003, **68**, 3327-3329.
27. We are actively examining this hypothesis and will report on it in due course.
28. G. Odian, *Principles of Polymerization*, John Wiley & Sons, Inc., Hoboken, New Jersey, 2004.
29. B. Sanz, N. Ballard, Á. Marcos-Fernández, J. M. Asua and C. Mijangos, *Polymer*, 2018, **140**, 131-139.

30. A. J. Brandolini and D. D. Hills, *NMR spectra of polymers and polymer additives*, CRC press, 2000.
31. N. Bloembergen, E. M. Purcell and R. V. Pound, *Phys. Rev.*, 1948, **73**, 679-712.
32. T. Yamamoto, W. Yamada, M. Takagi, K. Kizu, T. Maruyama, N. Ooba, S. Tomaru, T. Kurihara, T. Kaino and K. Kubota, *Macromolecules*, 1994, **27**, 6620-6626.
33. F. F. Cleveland and M. J. Murray, *J. Am. Chem. Soc.*, 1940, **62**, 3185-3188.
34. K. Roy, S. Kayal, F. Ariese, A. Beeby and S. Umapathy, *J. Chem. Phys.*, 2017, **146**, 064303.
35. J. N. Willis, M. T. Ryan, F. L. Hedberg and H. Rosenberg, *Spectrochimica Acta Part A: Molecular Spectroscopy*, 1968, **24**, 1561-1572.
36. J. Ma, A. P. Kalenak, A. G. Wong-Foy and A. J. Matzger, *Angew. Chem., Int. Ed.*, 2017, **56**, 14618-14621.
37. C. Levanda, K. Bechgaard and D. O. Cowan, *J. Org. Chem.*, 1976, **41**, 2700-2704.
38. K. Masahiro, M. Izumi, K. Motomi, M. Yuichi and S. Hirotoshi, *Chem. Lett.*, 1988, **17**, 1037-1040.
39. G. M. Brown, T. J. Meyer, D. O. Cowan, C. LeVanda, F. Kaufman, P. V. Roling and M. D. Rausch, *Inorg. Chem.*, 1975, **14**, 506-511.
40. B. J. Holliday and T. M. Swager, *Chem. Commun.*, 2005, 23-36.
41. D. M. D'Alessandro and F. R. Keene, *Dalton Trans.*, 2006, 1060-1072.